




Stage-Dependent Biomarker Changes in Spinocerebellar Ataxia Type 3

Jennifer Faber, MD ^{1,2}
 Moritz Berger, PhD,³ Carlo Wilke, MD ⁴
 Jeannette Hubener-Schmid, PhD ⁵,
 Tamara Schaprian, MSc,¹
 Magda M. Santana, PhD,^{6,7}
 Marcus Grobe-Einsler, MD,^{1,2}
 Demet Onder, MD,^{1,2} Berkan Koyak, MD,^{1,2}
 Paola Giunti, MD,^{8,9}
 Hector Garcia-Moreno, MD,^{8,9}
 Cristina Gonzalez-Robles, MD,^{8,9}
 Manuela Lima, PhD,¹⁰
 Mafalda Raposo, PhD,^{10,11}
 Ana Rosa Vieira Melo, MSc,¹⁰
 Luís Pereira de Almeida, PhD ^{6,7},
 Patrick Silva, MSc,^{6,7,12}
 Maria M. Pinto, MSc,^{7,8,12}
 Bart P. van de Warrenburg, MD, PhD,¹³
 Judith van Gaalen, MD,^{13,14}
 Jeroen de Vries, MD,¹⁵ Gulin Oz, PhD ¹⁶

James M. Joers, PhD,¹⁶
 Matthis Synofzik, MD ^{4,17}
 Ludger Schols, MD,^{4,17} Olaf Riess, MD,⁵
 Jon Infante, MD,^{18,19} Leire Manrique, MD,¹⁸
 Dagmar Timmann, MD,²⁰
 Andreas Thieme, MD,²⁰
 Heike Jacobi, MD ²¹
 Kathrin Reetz, MD ^{22,23}
 Imis Dogan, PhD,^{22,23}
 Chiadikaobi Onyike, MD,²⁴
 Michal Povazan, PhD,²⁵
 Jeremy Schmahmann, MD,²⁶
 Eva-Maria Ratai, PhD,²⁷
 Matthias Schmid, PhD,^{1,3} and
 Thomas Klockgether, MD^{1,2}

Spinocerebellar ataxia type 3/Machado–Joseph disease is the most common autosomal dominant ataxia. In view of the development of targeted therapies, knowledge of early biomarker changes is needed. We analyzed cross-sectional data of 292 spinocerebellar ataxia type 3/Machado–Joseph disease mutation carriers. Blood concentrations of mutant ATXN3 were high before and after ataxia onset, whereas neurofilament light deviated from normal 13.3 years before onset. Pons and cerebellar white matter volumes decreased and deviated from normal 2.2 years and 0.6 years before ataxia onset. We

From the ¹German Center for Neurodegenerative Diseases (DZNE), Bonn, Germany; ²Department of Neurology, University Hospital Bonn, Bonn, Germany; ³University of Bonn, Medical Faculty, Institute for Medical Biometry, Informatics, and Epidemiology, Bonn, Germany; ⁴German Center for Neurodegenerative Diseases (DZNE), Tübingen, Germany; ⁵Institute for Medical Genetics and Applied Genomics, University of Tuebingen, Tuebingen, Germany; ⁶Center for Neuroscience and Cell Biology (CNC), University of Coimbra, Coimbra, Portugal; ⁷Center for Innovative in Biomedicine and Biotechnology (CIBB), University of Coimbra, Coimbra, Portugal; ⁸Ataxia Centre, Department of Clinical and Movement Neurosciences, UCL Queen Square Institute of Neurology, University College London, London, UK; ⁹Department of Neurogenetics, National Hospital for Neurology and Neurosurgery, University College London Hospitals NHS Foundation Trust, London, UK; ¹⁰Faculdade de Ciências e Tecnologia, Universidade dos Açores, Ponta Delgada, Portugal; ¹¹Instituto de Biologia Molecular e Celular (IBMC), Instituto de Investigação e Inovação em Saúde (i3S), Universidade do Porto, Porto, Portugal; ¹²Faculty of Pharmacy, University of Coimbra, Coimbra, Portugal; ¹³Department of Neurology, Donders Institute for Brain, Cognition, and Behaviour, Radboud University Medical Center, Nijmegen, the Netherlands; ¹⁴Department of Neurology, Rijnstate Hospital, Arnhem, the Netherlands; ¹⁵University Medical Center Groningen, Neurology, Groningen, the Netherlands; ¹⁶Center for Magnetic Resonance Research, Department of Radiology, University of Minnesota, Minneapolis, MN, USA; ¹⁷Division Translational Genomics of Neurodegenerative Diseases, Hertie Institute for Clinical Brain Research & Center of Neurology, University of Tübingen, Tübingen, Germany; ¹⁸University Hospital Marqués de Valdecilla-IDIVAL, Santander, Spain; ¹⁹Centro de investigación biomédica en red de enfermedades neurodegenerativas (CIBERNED), Universidad de Cantabria, Santander, Spain; ²⁰Department of Neurology and Center for Translational Neuro- and Behavioral Sciences (C-TNBS), University Hospital Essen, University of Duisburg-Essen, Duisburg, Germany; ²¹Department of Neurology, University Hospital of Heidelberg, Heidelberg, Germany; ²²Department of Neurology, RWTH Aachen University, Aachen, Germany; ²³JARA-BRAIN Institute Molecular Neuroscience and Neuroimaging, Research Centre Juelich GmbH and RWTH Aachen University, Aachen, Germany; ²⁴Department of Psychiatry and Behavioral Sciences, Johns Hopkins University School of Medicine, Baltimore, MD, USA; ²⁵Johns Hopkins University School of Medicine, Baltimore, MD, USA; ²⁶Ataxia Center, Laboratory for Neuroanatomy and Cerebellar Neurobiology, Massachusetts General Hospital and Harvard Medical School, Boston, MA, USA; and ²⁷Massachusetts General Hospital, Department of Radiology, A. A. Martinos Center for Biomedical Imaging and Harvard Medical School, Charlestown, MA, USA

Address correspondence to Dr Jennifer Faber, German Center for Neurodegenerative Diseases (DZNE), Venusberg-Campus 1, 53127 Bonn, Germany. E-mail: jennifer.faber@dzne.de

Additional supporting information can be found in the online version of this article.

Received Apr 16, 2023, and in revised form Nov 9, 2023. Accepted for publication Nov 9, 2023.

View this article online at wileyonlinelibrary.com. DOI: 10.1002/ana.26824.

propose a staging model of spinocerebellar ataxia type 3/Machado–Joseph disease that includes a biomarker stage characterized by objective indicators of neurodegeneration before ataxia onset.

ANN NEUROL 2024;95:400–406

Introduction

Spinocerebellar ataxia type 3/Machado–Joseph disease (SCA3) is the most common autosomal dominantly inherited adult-onset ataxia disease worldwide with a progressive course leading to increasing disability and premature death. It is caused by unstable expansions of polyglutamine encoding CAG repeats, resulting in the formation of the abnormally elongated disease protein ATXN3.¹ Targeted therapies for SCA3 are being developed, and first safety trials of an antisense oligonucleotides have been initiated (<https://clinicaltrials.gov>, NCT05160558, NCT05822908). Future, preventive trials including SCA3 mutation carriers before ataxia onset are a realistic option. For the design of such trials, a thorough understanding of the dynamics of biomarkers that reflect the cascade of pathological events associated with SCA3 is a crucial prerequisite.

We analysed a large cross-sectional dataset of SCA3 mutation carriers ranging from the early phase before ataxia onset to the late advanced phase. Our aim was to delineate fluid and magnetic resonance imaging (MRI) biomarker changes in relation to ataxia manifestation that reflect key pathological changes of SCA3 and are known to be abnormal before ataxia onset; namely, ATXN3, neurofilament light (NFL), as well as MRI-derived pons and cerebellar volumes.^{2–10} By using a two-step regression analysis considering clinical, as well as fluid and imaging biomarker data, we were for the first time able to propose a staging model of SCA3.

Materials and Methods

Study Participants

This prospective, longitudinal, observational cohort study is carried out at 14 sites in 5 European countries and the USA. Participants of the European Spinocerebellar Ataxia Type 3/Machado–Joseph Disease Initiative (ESMI) cohort undergo annual standardized assessment, including a clinical examination and biosampling. MRI is carried out at 11 sites. SCA3 mutation carriers, their first-degree relatives, and healthy controls (HC) are eligible for inclusion. The study protocol is available under the following link: <https://idsn.dzne.de/esmi/study-protocols>.

For this analysis, we used cross-sectional data of 292 SCA3 mutation carriers and 108 healthy controls, of whom at least one fluid or MRI biomarker result was available at January 31, 2022. The ESMI consortium previously published individual biomarker data separately, and the present analysis is largely based on the combination of these data.^{3,5,8} The study was approved by the local

ethics committees. Written informed consent according to the Declaration of Helsinki was obtained from all participants.

Assessments

We used the Scale for the Assessment and Rating of Ataxia (SARA)¹¹ to assess the presence and severity of ataxia. Manifest ataxia was defined by a score of ≥ 3 .

Using a single molecule counting immunoassay, we measured plasma concentrations of expanded ATXN3.³ Serum concentrations of NFL were determined with an ultrasensitive single-molecule array assay.⁵ One single outlier with a value of NFL 4-fold higher than all other participants was excluded.

T1-weighted MRIs were acquired using a magnetization-prepared rapid gradient-echo sequence (TR = 2,500 ms, TE = 4.37 ms, TI = 1,100 ms, flip angle = 7 deg, FOV 256 × 256 mm, 192 slices with a voxel size of 1 mm isotropic) on Siemens 3T scanners (Siemens Medical Systems, Erlangen, Germany). Volumes of the pons, cerebellar white matter (CWM), and cerebellar grey matter (CGM)⁷ were measured and normalized by each participant's total intracranial volume.

In 243 study participants from whom DNA samples were available, repeat lengths of the expanded and normal alleles were centrally determined. For 43 participants, information about repeat lengths was taken from medical records; for 6 participants, no information was available.

Age of ataxia onset was defined as the reported first occurrence of gait disturbances. A total of 47 SCA3 mutation carriers did not yet experience gait disturbances (right-censored individuals). In a minority of patients ($n = 14$, 4.8%) with gait disturbance, information on the reported age of onset was missing (left-censored individuals). In these 61 SCA3 mutation carriers, the age of onset was estimated, as described below.

Statistical Analysis

Statistical analysis was carried out using R version 4.1.1 (R Core Team 2022; R: A Language and Environment for Statistical Computing; The R Foundation for Statistical Computing, Vienna, Austria).

To relate fluid and MRI biomarker data to the time from ataxia onset, we applied a conditional multiple imputation approach.¹² First, censored values of age of ataxia onset (or equivalently time from ataxia onset) were imputed fitting the parametric survival model by du Montcel et al.¹³ To account for interval censoring, covariate values were imputed with the conditional expectation for right-censored individuals (accounting for actual age), and with the unconditional expectation for left-censored individuals. Second, additive regression models were fitted for fluid and MRI biomarker values to the imputed covariate specifying a cubic P-spline with 6 B-spline basis functions and a second order difference penalty. This two-step procedure was repeatedly applied to 1,000 bootstrap samples from the original sample. Final estimates of the spline coefficients and associated variance estimates were then calculated by applying Rubin's rule.

For regression, NFL concentrations and MRI volumes were z-transformed with respect to age, as described before.⁸ As SARA scores and ATXN3 concentrations in healthy controls are close

to 0, no z-transformation was performed and the raw values were used. The analysis of the z-scores of NfL and MRI biomarkers was additionally adjusted for sex and site in multivariable regression models, and the analysis of ATXN3 and SARA for sex, sites, and age. To test for confounding effects of sex and site, and age, if applicable, a Bonferroni–Holm correction was applied.

Based on these regression models, we defined the carrier, biomarker, and ataxia stage. For a detailed description, we refer to the results section. Fluid and imaging biomarker values, as well as SARA sum scores, were compared between the three stages using one-way ANOVA followed by pairwise comparisons using Tukey's test.

Results

A total of 57 SCA3 mutation carriers before ataxia onset (35 women, mean age 35.5 years standard deviation [SD] 9.0), mean time from ataxia onset -10.1 years [SD 8.6]), 235 ataxic SCA3 mutation carriers (109 women, mean age 51.3 years [SD 11.3], mean time from ataxia onset 11.2 years [SD 7.8]), and 108 healthy controls (59 women, mean age 46.1 years [SD 14.0]) were included. MRI results, ATXN3 concentrations, and NfL levels were available in 161 (116 SCA3, 45 HC), 134 (122 SCA3, 12 HC), and 327 participants (239 SCA3, 88 HC), respectively, with an overlap between all 3 markers in 38 participants (33 SCA3, 5 HC), between ATXN3 and MRI in 39 (34 SCA3, 5 HC), between NfL and MRI in 96 (70 SCA3, 26 HC), and between ATXN3 and NfL in 115 participants (103 SCA3, 12 HC).

Changes of SARA scores, fluid biomarker levels, and MRI volumes of SCA3 mutation carriers in relation to the time from ataxia onset are shown in Figure 1. Overlap of the NfL 95% CIs of SCA3 mutation carriers with the interval of mean ± 2 SD of controls ended 13.3 years before onset. The overlap of pons and CWM volumes with controls ended 2.2 years (pons) and 0.6 years (CWM) before ataxia onset. CGM volume only slightly decreased and stayed within the ± 2 SD range around the mean of controls during the entire disease course. Multivariable confounding analyses showed no evidence for an effect of sex and site for the MRI biomarker and NfL, and of sex, site, and age for ATXN3 and SARA.

Based on the temporal sequence of biomarker changes, we defined the following disease stages. First, the carrier stage includes mutation carriers before ataxia onset without significant biomarker abnormalities other than the presence of mutant ATXN3 (SARA <3 and NfL z-score <2). We chose NfL as a criterion, as the preceding analysis showed that levels of NfL were the first of the studied biomarkers to change. Second, the biomarker stage includes mutation carriers before ataxia onset with significant biomarker changes in the absence of ataxia

(SARA <3 and NfL z-score ≥ 2). Third, the ataxia stage includes ataxic mutation carriers, defined by SARA ≥ 3 (Figure 2). Changes of SARA and the analyzed biomarkers in each stage are shown in Figure 3.

Discussion

Using cross-sectional data from 292 SCA3 mutation carriers, we estimated the sequence and extent of fluid and imaging biomarker changes along the disease course. Based on the observed changes, we drafted a staging model of SCA3 that includes an initial asymptomatic carrier stage followed by the biomarker stage characterized by absence of ataxia, but changes of NfL, as well as pons and cerebellar white matter volumes, finally leading into the ataxia stage, defined by manifest ataxia.¹⁴

This study had a number of limitations, the most important of which was its cross-sectional design. Even though ESMI is one of the largest SCA3 cohorts worldwide, the data volume, in particular of biomarkers, was still limited, resulting in only a few individuals in which all biomarkers were concurrently obtained. As MRI was only conducted at select sites, brain volume data were available of less than half of the participants, resulting in increased variability. Enrollment of mutation carriers from regions with significant disease cluster, such as the Azores, and from non-cluster regions, is a potential source of variability that might affect the modeling. However, an analysis of possible confounders did not show an effect of the study site. Additional sources of variability include potential inaccuracy of the estimated age of ataxia onset, and imperfect matching of the control population. Supplementation by longitudinal data and merging with data from other cohorts is therefore needed to corroborate our results.

Mutant ATXN3 was not used as a criterion for the definition of the biomarker stage, as concentrations were highly detectable throughout the entire disease course, characterizing it as a trait rather than a progression biomarker. The rise of NfL marks the first currently detectable damage to the nervous system in SCA3 and preceded ataxia onset by 11.9 years. This agrees with previous reports on NfL data of ESMI participants,^{2,5} as well as findings in other cohorts.^{15,16} Consequently, we used NfL as a criterion to define the biomarker stage in individuals prior to ataxia onset. Although NfL is supposed to reflect the rate of degeneration,⁵ volume loss rather represents the cumulated result of degeneration, explaining why volume loss followed the rise of NfL.¹⁵ As pons and CWM volumes showed a continuous decrease, and deviated from normal 2.0 and 0.3 years before ataxia onset, they may be considered for the stratification of mutation carriers close to the clinical onset. The prominent white matter loss is

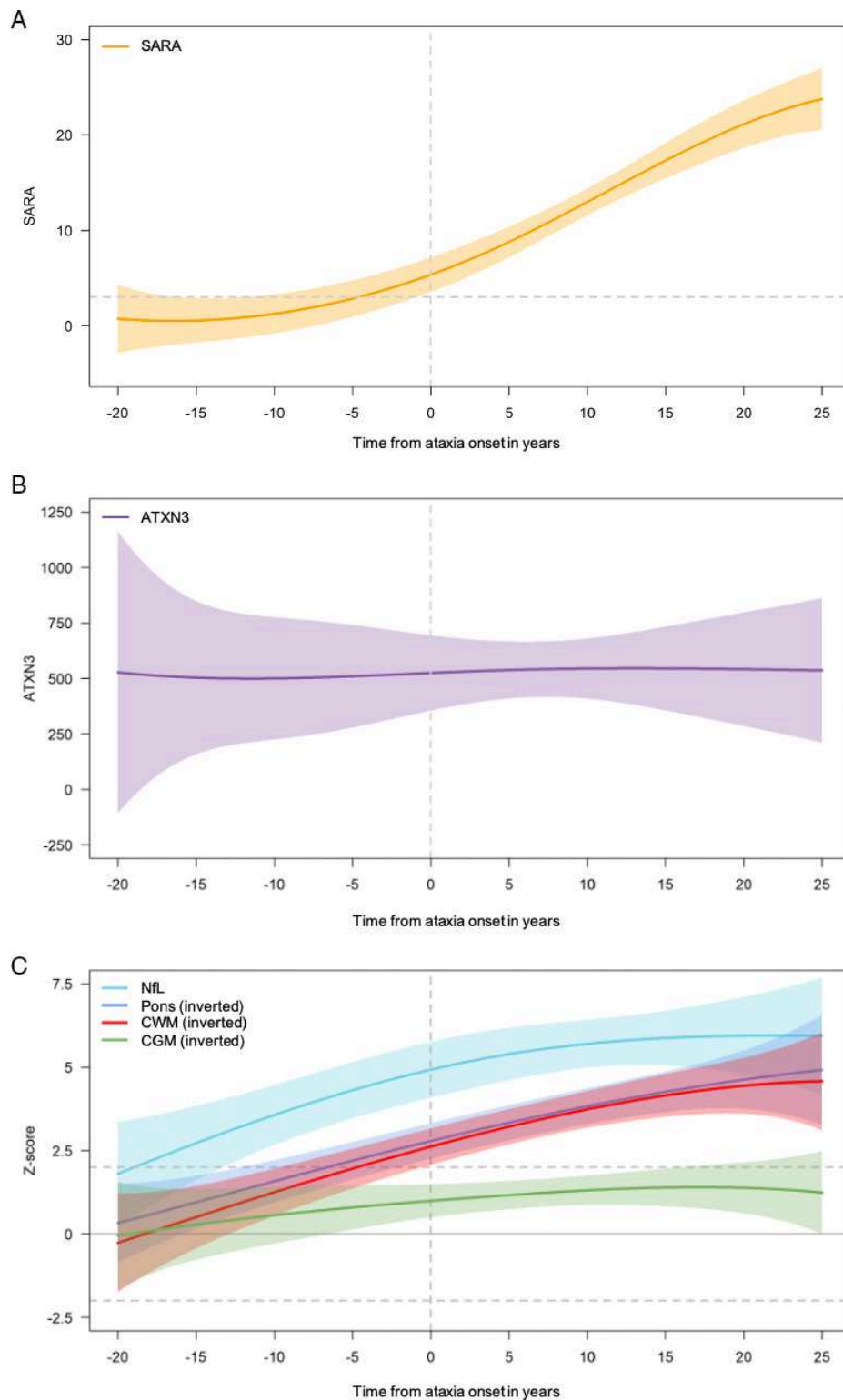


FIGURE 1: Scale for the Assessment and Rating of Ataxia (SARA) scores, fluid, and MRI biomarker data in spinocerebellar ataxia type 3/Machado–Joseph disease mutation carriers in relation to time from ataxia onset. Data were analyzed with additive regression models on a time scale defined by ataxia onset. The time of ataxia onset is shown by a vertical dashed line in all graphs. The estimated 95% confidence intervals are shown by the shaded areas around the curves. (A) SARA sum score. The SARA cut-off of 3 defining manifest ataxia is given as a dashed horizontal line. (B) Plasma concentrations of elongated ATXN3. Data are given in ng/ml. (C) Serum concentrations of neurofilament light (NfL), magnetic resonance imaging volumes of the pons, cerebellar white matter (CWM), and gray matter (CGM). Data were z-transformed in relation to healthy controls of same age. The y-axis of volume values is inverted for better comparability of volume loss and NfL increase. The mean of healthy controls is given as a horizontal line, the 1 SD range by dashed lines, and the 2 SD range by dotted lines.

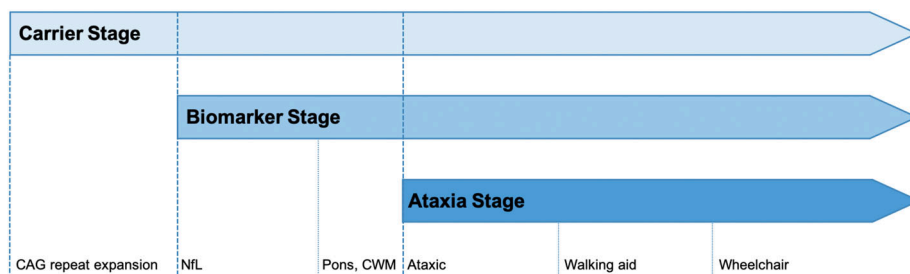


FIGURE 2: Staging model of spinocerebellar ataxia type 3/Machado–Joseph disease. Proposed staging model of spinocerebellar ataxia type 3/Machado–Joseph disease based on the studied fluid and magnetic resonance imaging biomarker data. The model includes an initial asymptomatic carrier stage followed by the biomarker stage defined by the absence of ataxia, but a significant rise of neurofilament light (NFL). The biomarker stage leads into the ataxia stage, which is defined by manifest ataxia. Following previous suggestions, the ataxia stage is further subdivided into three substages defined by milestones of gait deterioration.¹⁴ CGM = cerebellar gray matter; CWM = cerebellar white matter.

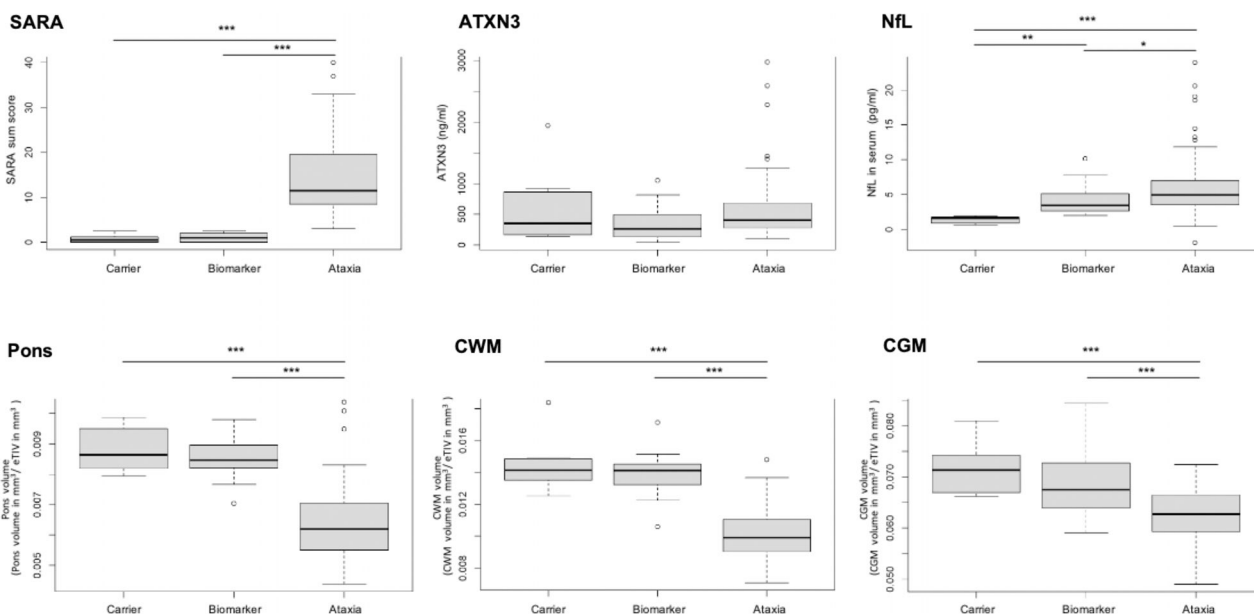


FIGURE 3: Scale for the Assessment and Rating of Ataxia (SARA) scores, fluid and magnetic resonance imaging biomarker data in the carrier, biomarker, and ataxia stage of spinocerebellar ataxia type 3/Machado–Joseph disease. Data were analyzed with one-way ANOVA followed by pairwise comparisons using Tukey's test * $p < 0.01$; ** $p < 0.001$. CGM = cerebellar grey matter; CWM = cerebellar white matter; eTIV = estimated intracranial volume; NfL = neurofilament light.

in line with autopsy and previous MRI findings that show relative sparing of cerebellar cortex in SCA3.^{17–19} Moreover, it is in line with observations of early oligodendrocyte pathology in mouse models of SCA3.²⁰

The present data allowed for the first time to draft a data-driven model of disease stages for SCA3 similar to that recently presented for Huntington's disease.²¹ Further studies including additional fluid and imaging biomarker data, such as MR spectroscopy and diffusion imaging,⁶ may allow to further subdivide the biomarker stage. The present staging model of SCA3 is to be considered as a first draft that needs to be further refined and extended based on more data and broad consensus. Nevertheless, it provides a robust framework for further studies aiming at elaboration and differentiation of a staging model of SCA3.

Acknowledgments

T.K., M.S., L.S., J.L., and B.vdW. are members of the European Reference Network for Rare Neurological Diseases (ERN-RD, project number 739510). The ESMI consortium acknowledges Ruth Hossinger for the project management of the ESMI project and for all contributions made toward the success of this project. This publication is an outcome of ESMI, an EU Joint Program – Neurodegenerative Disease Research (JPND) project (see www.jpnd.eu). The project is supported through the following funding organisations under the aegis of JPND: Germany, Federal Ministry of Education and Research (BMBF; funding codes 01ED1602A/B); Netherlands, The Netherlands Organization for Health Research and Development; Portugal, Fundação para a

Ciência e Tecnologia (funding code JPCOFUND/0002/2015); United Kingdom, Medical Research Council (MR/N028767/1). This project has received funding from the European Union's Horizon 2020 research and innovation program under grant agreement No. 643417. The Azores ESMI Network is currently supported by the Regional Government (Fundo Regional para a Ciência e a Tecnologia-FRCT), under the PRO-SCIENTIA program. At the USA sites, this work was in part supported by the National Ataxia Foundation and the National Institute of Neurological Disorders and Stroke (NINDS) grant R01NS080816. The Center for Magnetic Resonance Research is supported by the National Institute of Biomedical Imaging and Bioengineering (NIBIB) grant P41 EB027061, the Institutional Center Cores for Advanced Neuroimaging award P30 NS076408 and S10 OD017974 grant. T.K. received research support from the Bundesministerium für Bildung und Forschung (BMBF), the National Institutes of Health (NIH) and Servier. J.F. received funding as a Fellow of the Hertie Network of Excellence in Clinical Neuroscience. M.R. is supported by FCT (CEECIND/03018/2018). B.vdW. received funding from ZonMw, NWO, Gossweiler Foundation, Brugling Fonds, Radboudumc, Hersenstichting, and Christina Foundation. C.O. received funding from NINDS #U01 NS104326; the National Ataxia Foundation; and Robert and Nancy Hall Brain Research Fund. J.S. is supported in part by the National Ataxia Foundation, the Raynor Cerebellum Project, and the MINDlink Foundation. J.J. received grant support from NIH and Friedrich's Ataxia Research Alliance (FARA). A.T. received research grants from the University Medicine Essen Clinician Scientist Academy (UMEA)/Deutsche Forschungsgemeinschaft (DFG, grant number: FU356/12-2). At the Portuguese sites, M.M.S. and L.P.A. received funding from European Regional Development Fund (ERDF), through the Centro 2020 Regional Operational Program, and through the COMPETE 2020 – Operational Program for Competitiveness and Internationalization; and Portuguese national funds via FCT – Fundação para a Ciência e a Tecnologia, under the projects: CENTRO-01-0145-FEDER-181240, 2022.06118.PTDC, UIDB/04539/2020, UIDP/04539/2020, LA/P/0058/2020, ViraVector (CENTRO-01-0145-FEDER-022095), Fighting Sars-CoV-2 (CENTRO-01-01D2-FEDER-000002), BDforMJD (CENTRO-01-0145-FEDER-181240 & 2022.06118.PTDC), ModelPolyQ2.0 (CENTRO-01-0145-FEDER-181258), and MJDEDIT (CENTRO-01-0145-FEDER-181266); ARDAT under the IMI2 JU Grant agreement No 945473 supported by the European Union's H2020 program and EFPIA; by the American Portuguese Biomedical Research Fund (APBRF), National Ataxia Foundation, and the Richard Chin and Lily Lock

Machado-Joseph Disease Research Fund. P.S. and M.M.P. were supported by FCT under the fellowship grant SFRH/BD/148451/2019, and 2019 and 2022.11089.BD. C.W. was supported by the Clinician Scientist Program of the Medical Faculty Tübingen (480-0-0). P.G. is supported by the National Institute for Health Research University College London Hospitals Biomedical Research Center UCLH. P.G. also receives support from the North Thames CRN. P.G. and H.G-M work at University College London Hospitals/University College London, which receives a proportion of funding from the Department of Health's National Institute for Health Research Biomedical Research Center's funding scheme. P.G. received funding from the Medical Research Council (MR/N028767/1) and CureSCA3 in support of H.G-M's work.

Author Contributions

J.F. and T.K. contributed to the conception and design of the study. J.F., M.B., T.K., M.S., C.W., J.H-S., T.S., M.M.S., M.G-E., D.O., B.K., P.G., H.C-M., C.G-R., M.L., M.R., A.M., L.P.A., P.S., M.P., B.vdW., J.G., J.V., G.O., M.S., L.S., O.R., J.I., L.M., D.T., A.T., H.J., K.R., I.D., C.O., M.P., J.S., and E-M.R. contributed to the acquisition and analysis of the data. J.F., T.K., M.B., and M.Sch. contributed to the drafting of the text or preparing the figures.

Potential Conflicts of Interest

G.O. consults for IXICO Technologies Limited, which provides neuroimaging services and digital biomarker analytics to biopharmaceutical firms conducting clinical trials for SCAs, and receives research support from Biogen, which develops therapeutics for SCAs. M.S. received consultancy honoraria from Ionis, UCB, Prevail, Orphazyme, Servier, Reata, GenOrph, AviadoBio, Biohaven, Zevra, and Lilly, all unrelated to the present manuscript. J.F. received consultancy fees from Vico Therapeutics, unrelated to the present manuscript. T.K. received consulting fees within the past 24 months from UCB and Vico Therapeutics. L.S. received consultancy honoraria from Vico Therapeutics and Novartis unrelated to the present manuscript. LPA research group has private funding from PTC Therapeutics, Uniqure, Wave life Sciences, Servier, Blade Therapeutics, and Hoffmann-La Roche AG outside the submitted work. C.O. served as consultant for Acadia, Eisai, Ostuka, and Reata, and received funding from Alector, Transposon, and Denali for work focused on hereditary frontotemporal dementias. P.G. received honoraria for grants and consultancies from Reata Pharmaceuticals and Vico therapeutics, and consultancy work

for PTC Therapeutics, all unrelated with the submitted work.

References

- Paulson H. Machado-Joseph disease/spinocerebellar ataxia type 3. *Handb Clin Neurol* 2012;103:437–449.
- Garcia-Moreno H, Prudencio M, Thomas-Black G, et al. Tau and neurofilament light-chain as fluid biomarkers in spinocerebellar ataxia type 3. *Eur J Neurol* 2022;29:2439–2452.
- Hubener-Schmid J, Kuhlbrodt K, Peladan J, et al. Polyglutamine-expanded Ataxin-3: a target engagement marker for spinocerebellar ataxia type 3 in peripheral blood. *Mov Disord* 2021;36:2675–2681.
- Li QF, Dong Y, Yang L, et al. Neurofilament light chain is a promising serum biomarker in spinocerebellar ataxia type 3. *Mol Neurodegener* 2019;14:39.
- Wilke C, Haas E, Reetz K, et al. Neurofilaments in spinocerebellar ataxia type 3: blood biomarkers at the preataxic and ataxic stage in humans and mice. *EMBO Mol Med* 2020;12:e11803.
- Chandrasekaran J, Petit E, Park YW, et al. Clinically meaningful magnetic resonance endpoints sensitive to Preataxic spinocerebellar ataxia types 1 and 3. *Ann Neurol* 2022;93:686–701.
- Faber J, Kugler D, Bahrami E, et al. CerebNet: a fast and reliable deep-learning pipeline for detailed cerebellum sub-segmentation. *Neuroimage* 2022;264:119703.
- Faber J, Schaprian T, Berkan K, et al. Regional brain and spinal cord volume loss in spinocerebellar ataxia type 3. *Mov Disord* 2021;36:2273–2281.
- Rezende TJR, de Paiva JLR, Martinez ARM, et al. Structural signature of SCA3: from presymptomatic to late disease stages. *Ann Neurol* 2018;84:401–408.
- Prudencio M, Garcia-Moreno H, Jansen-West KR, et al. Toward allele-specific targeting therapy and pharmacodynamic marker for spinocerebellar ataxia type 3. *Sci Transl Med* 2020;12:566.
- Schmitz-Hubsch T, du Montcel ST, Baliko L, et al. Scale for the assessment and rating of ataxia: development of a new clinical scale. *Neurology* 2006;66:1717–1720.
- Atem FD, Sampene E, Greene TJ. Improved conditional imputation for linear regression with a randomly censored predictor. *Stat Methods Med Res* 2019;28:432–444.
- Tezenas du Montcel S, Durr A, Rakowicz M, et al. Prediction of the age at onset in spinocerebellar ataxia type 1, 2, 3 and 6. *J Med Genet* 2014;51:479–486.
- Klockgether T, Ludtke R, Kramer B, et al. The natural history of degenerative ataxia: a retrospective study in 466 patients. *Brain* 1998;121:589–600.
- Coarelli G, Darios F, Petit E, et al. Plasma neurofilament light chain predicts cerebellar atrophy and clinical progression in spinocerebellar ataxia. *Neurobiol Dis* 2021;153:105311.
- Peng Y, Zhang Y, Chen Z, et al. Association of serum neurofilament light and disease severity in patients with spinocerebellar ataxia type 3. *Neurology* 2020;95:e2977–e2987.
- Koeppen AH. The neuropathology of spinocerebellar ataxia type 3/Machado-Joseph disease. *Adv Exp Med Biol* 2018;1049:233–241.
- Piccinin CC, Rezende TJR, de Paiva JLR, et al. A 5-year longitudinal clinical and magnetic resonance imaging study in spinocerebellar ataxia type 3. *Mov Disord* 2020;35:1679–1684.
- Chandrasekaran J, Petit E, Park YW, et al. Clinically meaningful MR endpoints sensitive to preataxic SCA1 and SCA3. *Ann Neurol* 2023;93:686–701.
- Schuster KH, Zalon AJ, Zhang H, et al. Impaired oligodendrocyte maturation is an early feature in SCA3 disease pathogenesis. *J Neurosci* 2022;42:1604–1617.
- Tabrizi SJ, Schobel S, Gantman EC, et al. A biological classification of Huntington's disease: the integrated staging system. *Lancet Neurol* 2022;21:632–644.